DOI: 10.1111/exd.12042
www.blackwellpublishing.com/EXD

A sprayable luminescent pH sensor and its use for wound imaging *in vivo*

Stephan Schreml[1], Robert J. Meier[2], Katharina T. Weiß[1], Julia Cattani[2], Dagmar Flittner[2], Sebastian Gehmert[3], Otto S. Wolfbeis[2], Michael Landthaler[1] and Philipp Babilas[1]

[1]Department of Dermatology, University Medical Center Regensburg, Regensburg, Germany; [2]Institute of Analytical Chemistry, Chemo- and Biosensors, University of Regensburg, Regensburg, Germany; [3]Department of Plastic Surgery, University Medical Center Regensburg, Regensburg, Germany

Correspondence: Philipp Babilas, MD or Stephan Schreml, MD, Department of Dermatology, University Medical Center Regensburg, Franz-Josef-Strauss-Allee 11, 93053 Regensburg, Germany, Tel.: +49-(0)941-944-9601, Fax: +49-(0)941-944-9611, e-mails: philipp.babilas@ukr.de; stephan@schreml.de

Abstract: Non-invasive luminescence imaging is of great interest for studying biological parameters in wound healing, tumors and other biomedical fields. Recently, we developed the first method for 2D luminescence imaging of pH *in vivo* on humans, and a novel method for one-stop-shop visualization of oxygen and pH using the RGB read-out of digital cameras. Both methods make use of semitransparent sensor foils. Here, we describe a sprayable ratiometric luminescent pH sensor, which combines properties of both these methods. Additionally, a major advantage is that the sensor spray is applicable to very uneven tissue surfaces due to its consistency. A digital RGB image of the spray on tissue is taken. The signal of the pH indicator (fluorescein isothiocyanate) is stored in the green channel (G), while that of the reference dye [ruthenium(II)-tris-(4,7-diphenyl-1,10-phenanthroline)] is stored in the red channel (R). Images are processed by rationing luminescence intensities (G/R) to result in pseudocolor pH maps of tissues, e.g. wounds.

Key words: cutaneous, luminescence, ratiometric, RGB imaging, skin

Accepted for publication 26 September 2012

Background

Impaired wound healing is an enormous medical and socio-economic issue (1). In contrast to the stepwise process of physiological healing (inflammation, proliferation and remodeling; 2,3), chronic wounds are trapped in a non-healing, mostly inflammatory, state. Basic biological parameters, such as oxygen (4), pH (5) and reactive oxygen species (ROS; 6–8), are known to affect healing. Extracellular signals govern tissue morphogenesis (9), which is essential for wound closure. Extracellular pH is one of these signals, and known to modify gene expression patterns of skin cells and bacteria (10,11), to regulate mRNA splicing patterns (12), to control cell proliferation/migration (13,14), to affect enzyme activity (e.g. matrix metalloproteinases) and epidermal homoeostasis (e.g. regulation of NHE1; 15,16), and to alter growth factor actions (17). Additionally, it is known that the fluid covering the wound surface is of great importance for healing (18–20). Taking all this into account, the study of pH on wound surfaces is of utmost interest.

Appropriate tools to study pH *in vivo* on humans are still missing. The pH glass electrode (21) only allows single-spot pH measurements, which are insufficient for studying heterogeneous tissue structures, such as chronic wounds. Recently, we described luminescent sensor foils for 2D imaging of pH and pO_2 *in vivo* (22–24). However, these sensor foils are sometimes not flexible enough to attach consistently to very uneven surfaces, which are often found in chronic wounds. The use of sensor sprays (25) may overcome this issue.

Questions addressed

The aim was to create a method for (photographic) luminescent imaging of pH values on very uneven tissue surfaces (e.g. wounds) *in vivo*. The sensor materials had to be (i) sprayable, (ii) strongly luminescent (adequate signal intensity), (iii) non-irritant and (iv) easily removable. Here we describe a sprayable luminescent sensor for imaging of pH values *in vivo* on humans.

Experimental design and results

Luminescent sensor particles

Fluorescein isothiocyanate (FITC, λ_{ex} 507 nm, λ_{em} 542 nm) was covalently linked to aminoethylcellulose (AC) to form pH indicator particles (FITC-AC; 23). The oxygen-sensitive probe ruthenium (II)-tris(4,7-diphenyl-1,10-phenanthroline;) ($Ru(dpp)_3$) was incorporated in oxygen-impermeable polyacrylonitrile (PAN) particles, which then served as reference particles ($Ru(dpp)_3$-PAN; λ_{ex} 468 nm, λ_{em} 605 nm; 23). For details, we refer to our methods papers (23,26).

Sensor fluid

A 10:2 ratio of FITC-AC/$Ru(dpp)_3$-PAN particles yielded suitable signal intensities for ratiometric imaging. Sensor particles were embedded in a mixture of Traumasept wound gel (Dr. August Wolff GmbH & Co. KG, Bielefeld, Germany) and water. No other solvents were used, making the mixture biocompatible for use on humans. An ideal ratio of gel and water was found at 3:1 v/v. At higher ratios, the sensor fluid was too viscous to keep it sprayable. At lower ratios, the viscosity was too low to create a relatively stable homogeneous layer. A sensor particle concentration of 10 mg/ml in the final fluid was found to work best.

Spray device

To apply the sensor on tissue, we used a commercial pump-action spray device as used for nasal sprays.

Study subjects

Written informed consent was obtained from the study subjects prior to measurements. The local ethics committee gave approval (No. 06/171), and we did all experiments in accordance with the declaration of Helsinki.

Imaging

Time-domain dual lifetime referencing (td-DLR; 23,27) can be used to visualize pH with these particles. However, to use a faster approach, we applied the RGB read-out of a commercial camera (22,28). A 460-nm LED array mounted on a commercial camera (22) was used to excite the luminophores. An RGB image of the sensor fluid on tissue was then acquired. The pH-dependent signal is stored in the green channel (G), and the pH-independent reference signal is stored in the red channel (R) of the RGB image. The ratio of G/R luminescence intensities gives a referenced pH signal for each pixel (22). The blue channel (B) does not contain relevant information in this setup.

In vivo calibration

The effect of pH on the combined green and red emissions can be seen in the pictures even with the naked eye (Fig. 1a). The RGB image was split into the three colour channels using ImageJ (http://rsbweb.nih.gov/ij/). The luminescence intensity of FITC-AC particles increases along with rising pH (Fig. 1b), whereas that of the reference particles [$Ru(dpp)_3$-PAN] remains constant (Fig. 1c). Data of the blue channel are not used in this setup. Ratios between the intensities in the green and the red channel (G/R) were calculated, and according pseudocolor images of pH (Fig. 1d) were created. We did a sigmoidal fit, and we solved the resulting equation for pH (Fig. 1e). This equation could then be used for pH calculations for each pixel.

In vivo application

To demonstrate that the sensor provides correct pH information *in vivo*, the sensor spray was applied to visualize two drops of buffer solutions (pH 4 and 9) on the volar forearm of a volunteer (Fig. 1f). Next, the sensor was used to visualize pH during physiological healing in a region of interest (ROI, Fig. S1) within a split skin donor site. pH decreased during the time course of wound closure (Fig. 1g–i, 23). Additionally, the heterogeneous pH distribution on an uneven chronic venous ulcer was visualized (Fig. 1j,k). After imaging, the sensor fluid was completely removed (Fig. S2) by wiping out the wound with sterile compresses soaked in Ringer's solution. There were no signs of irritation in the area of application. The capability to image pH variations in different wounds was also demonstrated (Fig. S3). Apart from these applications, the sensor was used to visualize pH changes induced by bacteria (Fig. S4), which often colonize chronic wounds.

Conclusion

The sprayable sensor enables a fast, straightforward visualization of pH *in vivo*. As water was used as solvent, the imaging process is painless and leaves wound healing unaffected. The sensor can be removed by water-based solutions. After image acquisition, picture transformations have to be done. These steps (white balancing, splitting in RGB channels, calculation of G/R-ratios, calibration curves and pseudocolor image processing) could be stored in a program on a digital camera, which would enable automatic, real-time pseudocolor pH image previews.

Targeting the pH of tumors is also a field of great interest (29). The striking similarities between chronic wound healing and can-

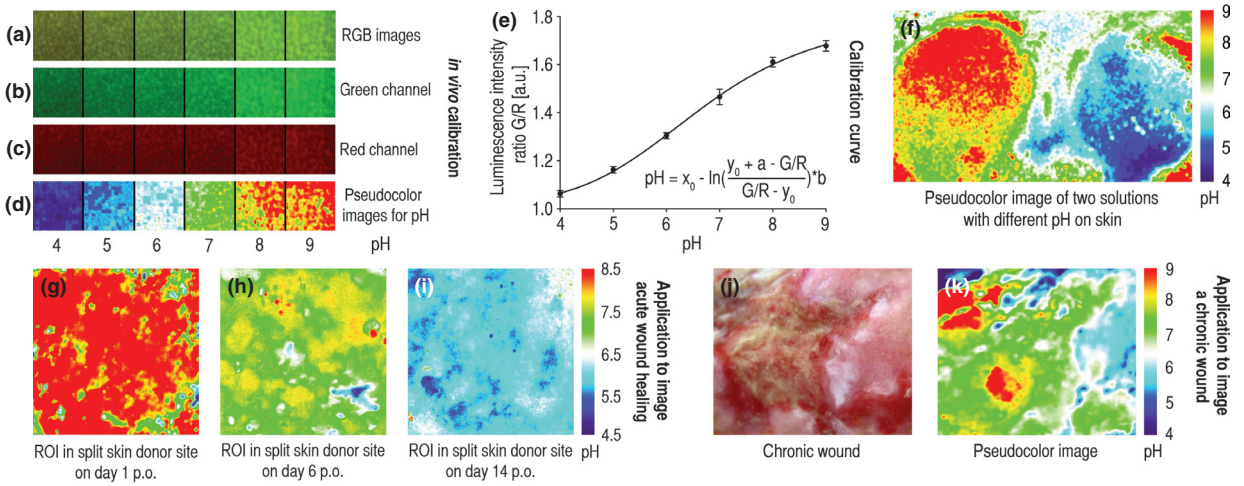

Figure 1. *Sensor Calibration and application in cutaneous wound healing.* (a) RGB images of the pH sensor at varying pH values. After splitting the images into the RGB (red-green-blue) channels, (b) the pH-dependent luminescence of FITC-AC (fluoresceinisothiocyanate on aminocellulose particles) in the green channel (G), and (c) the pH-independent luminescence of $Ru(dpp)_3$-PAN [ruthenium(II)-tris(4,7-diphenyl-1,10-phenanthroline) in polyacrylonitrile particles] in the red channel (R) are seen. The ratios between the intensities (G/R) give a referenced pH-signal, which is shown on a (d) pseudocolor scale. The (e) respective calibration curve allows to calculate pH by solving a sigmoidal fit equation for pH (triplicate samples, mean ± SD). For *in vivo* validation, (f) two drops of solutions with different pH (4 and 9) on the volar forearm of a volunteer were visualized. (g–i) The sensor spray was used to visualize physiological healing of a split skin donor site on the ventral thigh of a patient. A region of interest (ROI) was defined (Fig. S1), and measurements were performed on days 1, 6, and 14 after split skin harvesting. Mean pH values were 8.56 (day 1 postoperatively), 7.51 (day 6 postoperatively), and 6.23 (day 14 postoperatively). These values match the data we published using semitransparent sensor foils (see reference 23, ROI = region of interest, p.o. = postoperatively). (j) An uneven chronic venous ulcer on the lower leg of a patient is shown (without sensor). After application of the sprayable pH sensor with a commercial nasal spray device, a standard RGB image was taken (Fig. S2a). The sensor was then wiped off completely (Fig. S2b). Subsequently, the RGB image was split into the RGB channels. G/R ratios were created, and a (k) pseudocolor map of pH was computed using the equation obtained from sensor calibration (e). The bluish colors indicate surrounding intact (or nearly intact) skin. The green and red colors represent areas of sustained inflammation and partial granulation. When compared to physiological healing (g–i), the red areas exhibit the highest degree of inflammation.

cer (30) give rise to future applications of 2D pH sensors in studying tumor metabolism.

Acknowledgements

This work was supported by grants from the German Research Foundation DFG (grants BA3410/4–1 and WO669/9–1). Traumasept Wound Gel was supplied by Dr. August Wolff GmbH & Co. KG (Bielefeld, Germany).

Author contributions

S.S., R.J.M., O.S.W. and P.B. conceived the experiments. S.S., R.J.M., K.T.W., J.C. and D.F. performed the experiments. S.S., R.J.M. and D.F. analysed the data. S.S. and R.J.M. wrote the paper. S.G. helped to interpret data.

Conflict of interests

None declared.

References

1 Bickers D R, Lim H W, Margolis D *et al.* J Am Acad Dermatol 2006: **55**: 490–500.
2 Gurtner G C, Werner S, Barrandon Y *et al.* Nature 2008: **453**: 314–321.
3 Martin P. Science 1997: **276**: 75–81.
4 Schreml S, Szeimies R M, Prantl L *et al.* Br J Dermatol 2010: **163**: 257–268.
5 Schreml S, Szeimies R M, Karrer S *et al.* J Eur Acad Dermatol Venereol 2010: **24**: 373–378.
6 Dickinson B C, Chang C J. Nat Chem Biol 2011: **7**: 504–511.
7 Niethammer P, Grabher C, Look A T *et al.* Nature 2009: **459**: 996–999.
8 Yoo S K, Starnes T W, Deng Q *et al.* Nature 2011: **480**: 109–112.
9 Muller P, Schier A F. Dev Cell 2011: **21**: 145–158.
10 Bumke M A, Neri D, Elia G. Proteomics 2003: **3**: 675–688.
11 Olson E R. Mol Microbiol 1993: **8**: 5–14.
12 Borsi L, Balza E, Gaggero B *et al.* J Biol Chem 1995: **270**: 6243–6245.
13 Sharpe J R, Harris K L, Jubin K *et al.* Br J Dermatol 2009: **161**: 671–673.
14 Paradise R K, Lauffenburger D A, Van Vliet K J. PLoS One 2011: **6**: e15746.
15 Behne M J, Meyer J W, Hanson K M *et al.* J Biol Chem 2002: **277**: 47399–47406.
16 Hachem J P, Behne M, Aronchik I *et al.* J Invest Dermatol 2005: **125**: 790–797.
17 Goerges A L, Nugent M A. J Biol Chem 2003: **278**: 19518–19525.
18 Hinman C D, Maibach H. Nature 1963: **200**: 377–378.
19 Winter G D. Nature 1962: **193**: 293–294.
20 Winter G D, Scales J T. Nature 1963: **197**: 91–92.
21 Walpole G S. Biochem J 1914: **8**: 131–133.
22 Meier R J, Schreml S, Wang X D *et al.* Angew Chem Int Ed Engl 2011: **50**: 10893–10896.
23 Schreml S, Meier R J, Wolfbeis O S *et al.* Proc Natl Acad Sci U S A 2011: **108**: 2432–2437.
24 Schreml S, Meier R J, Wolfbeis O S *et al.* Exp Dermatol 2011: **20**: 550–554.
25 Fischer L H, Borisov S M, Schaeferling M *et al.* Analyst 2010: **135**: 1224–1229.
26 Borisov S M, Krause C, Arain S *et al.* Adv Mater 2006: **18**: 1511–1516.
27 Liebsch G, Klimant I, Krause C *et al.* Anal Chem 2001: **73**: 4354–4363.
28 Schaferling M. Angew Chem Int Ed Engl 2012: **51**: 3532–3554.
29 Neri D, Supuran C T. Nat Rev Drug Discov 2011: **10**: 767–777.
30 Arwert E N, Hoste E, Watt F M. Nat Rev Cancer 2012: **12**: 170–180.

Supporting Information

Additional Supporting Information may be found in the online version of this article:

Figure S1. Region of interest in a split skin donor site wound.

Figure S2. Demonstration of complete sensor removal.

Figure S3. Visualization of pH heterogeneity in wounds.

Figure S4. Visualization of bacteria-induced pH changes.

SUPPORTING INFORMATION

Schreml S *et al.*

A sprayable luminescent pH sensor and its use for wound imaging *in vivo*

Figure S1

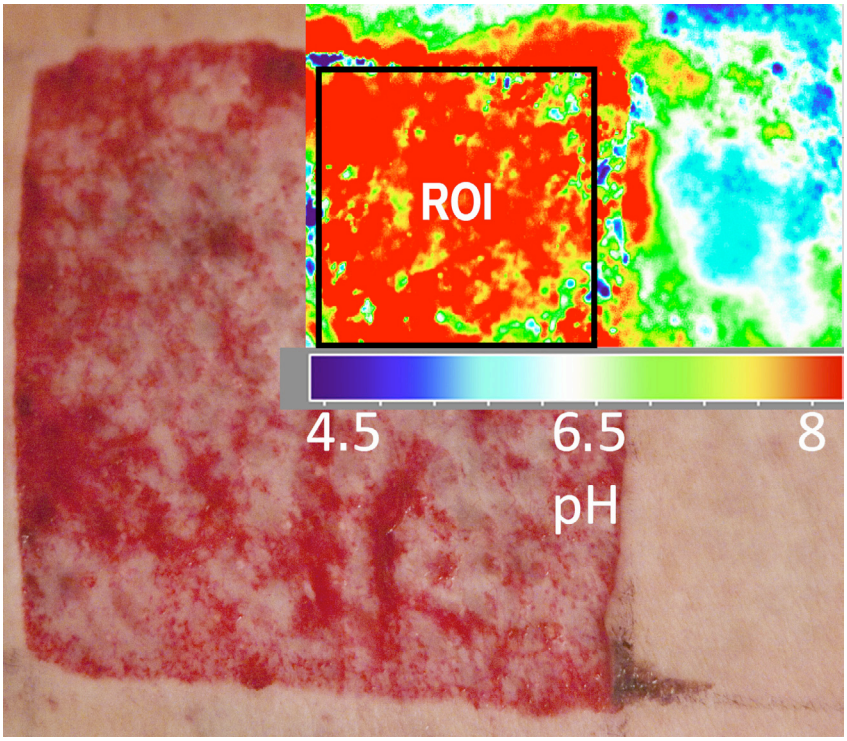

Figure S1: Region of interest in a split-skin donor site wound. To follow pH during the time course of physiological healing, a region of interest (ROI) was defined within a split skin donor site on the ventral thigh of a patient. Mean pH values and pseudocolor images (**Fig. 1g-i**) were then calculated from these ROIs.

Figure S2

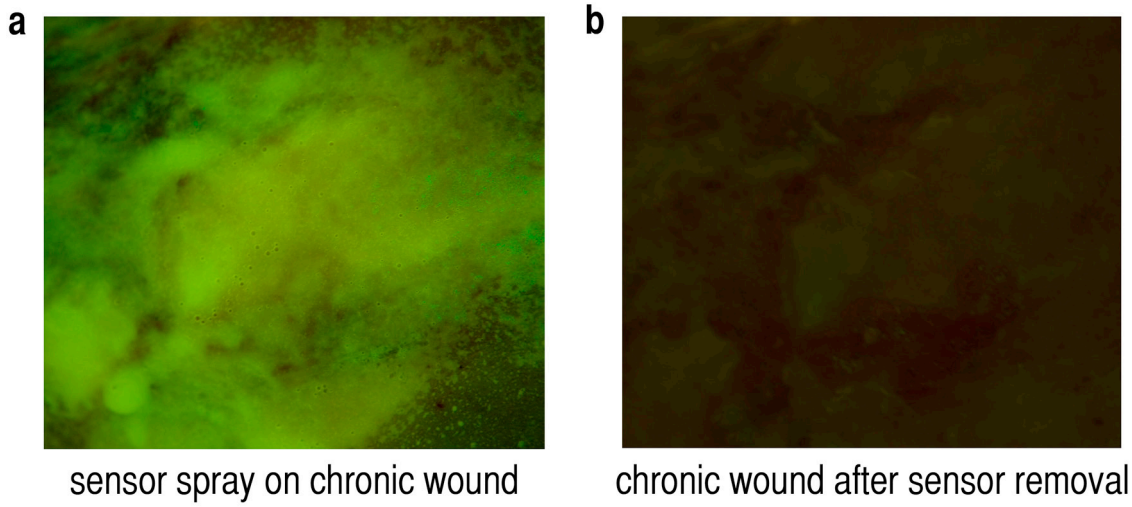

Figure S2: Demonstration of complete sensor removal. (**a**) After application of the sprayable pH sensor with a commercial nasal spray device, a standard RGB image under UV excitation was taken. (**b**) The sensor was then wiped off completely, and only weak background fluorescence from the wound surface was seen. No residual sensor particles were seen.

Figure S3

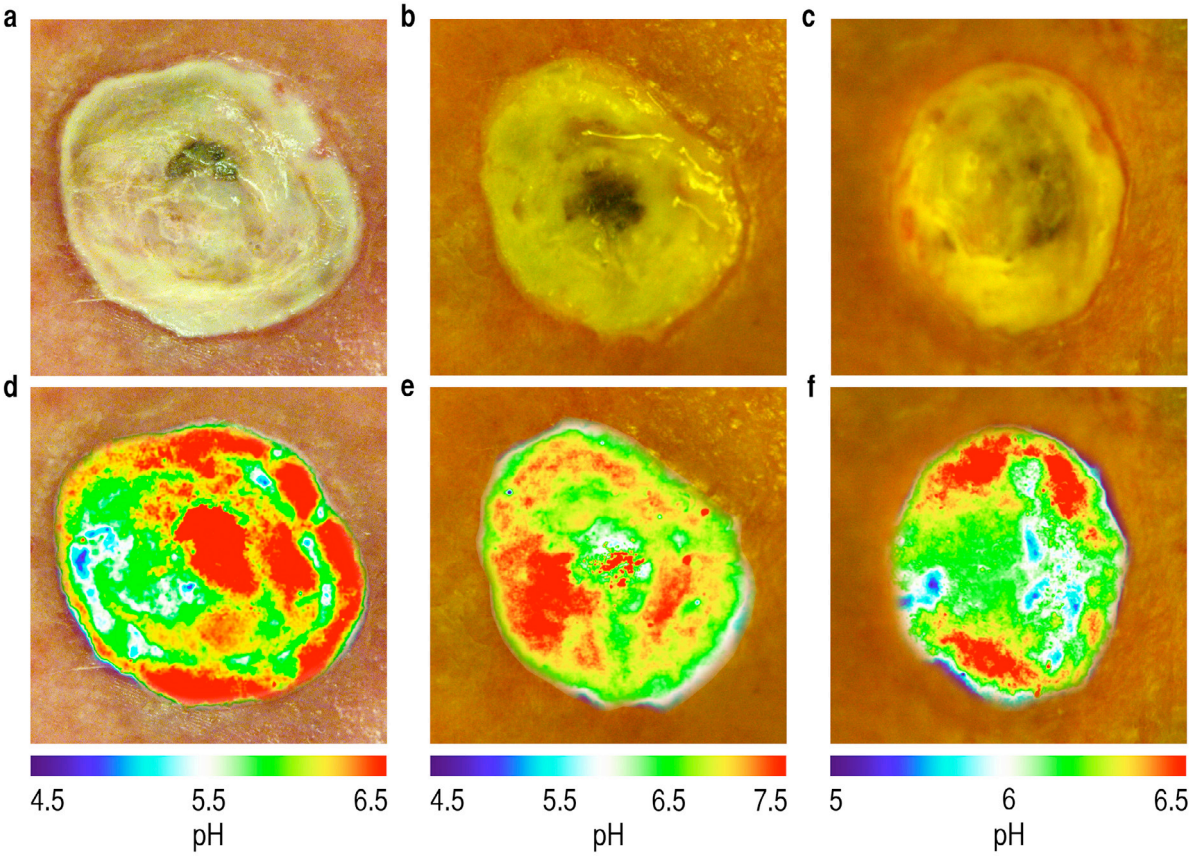

Figure S3: Visualization of pH heterogeneity in wounds. (**a-c**) The images show three vasculitic wounds of a woman (62 years). (**d-f**) The heterogeneous pH distribution within these wounds is shown. Areas with high pH are predominantly found close to the wound edges in this type of chronic wounds.

Figure S4

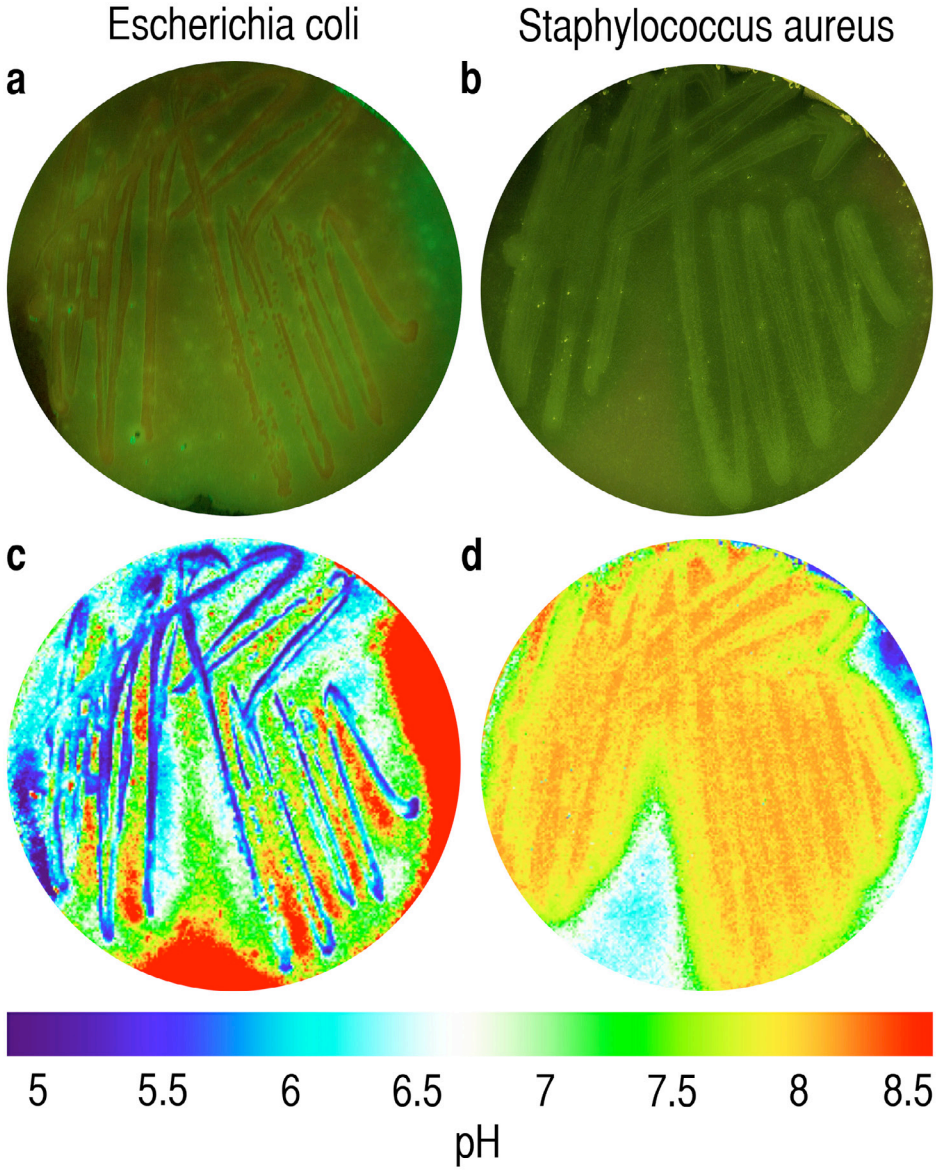

Figure S4: Visualization of bacteria-induced pH changes. (**a,b**) The images show bacterial culture plates with (**a**) Escherichia coli and (**b**) Staphylococcus aureus coated with sensor spray. (**c,d**) The bacteria-induced pH changes were visualized. Acid-producing Escherichia coli led to low pH values, while Staphylococcus aureus cultures predominantly showed higher pH values.